ISBN: 978-3-95450-247-9 ISSN: 2673-5490 doi: 10.18429/JACoW-IPAC2024-THPC36

SOLEIL II BOOSTER ROBUSTNESS AND EMITTANCE EXCHANGE

P. Schreiber*, P. Alexandre, F. Bouvet, S. Ducourtieux, R. Ben El Fekih, M.-A. Tordeux,
Synchrotron SOLEIL, Gif-sur-Yvette, France
Z. Bai, National Synchrotron Radiation Laboratory, USTC, Hefei, China

Abstract

For the injection into the SOLEIL II storage ring a beam with small transverse and longitudinal sizes is necessary, which requires the booster synchrotron to be upgraded. The new booster is designed as a 16 BA Higher-Order Achromat lattice with a small emittance of about 5 nm rad at 2.75 GeV. Robustness of the lattice has been studied with realistic errors in magnet alignment and calibration, but also taking into account specific errors as mismatch in the RF frequency and circumference error, as RF frequency is driven by the main storage ring. Also, power supply tracking errors have been considered and their reduction will be discussed. On top of these error studies an emittance exchange is performed to allow more flexibility in the injection parameters into the storage ring. Different methods are compared within the framework of a very realistic machine.

INTRODUCTION

SOLEIL, the French synchrotron light source, is currently preparing an upgrade to reduce the ring emittance down towards 85 pm rad [1–3]. Simulations show that a reduced emittance from the booster of about 5 nm rad together with a reduction in bunch length provides the necessary margin of injection error into the upgraded storage ring [4]. Both requirements call for the construction of an upgraded booster [5]. Studies on the new booster performance are ongoing [6] and the main parameters are given in [6] and briefly recounted in Table 1. As with any new construction of a storage ring or a booster, some errors in terms of alignment, calibration, frequency of the RF system, etc., are expected and are taken into account. To this end, simulations using the accelerator toolbox (AT) [7,8] and simulated commissioning (SC) [9] were performed.

ROBUSTNESS

For a successful commissioning of the booster, a robustness study is being performed. To this end, various errors have been estimated with the values given in Table 2. The alignment errors have been optimised in agreement with the alignment and survey team to be both, realistic to achieve, and suitable for beam dynamics.

The error on the frequency of the RF system was assumed to be quite large. As the storage ring and booster share a master clock, a relative circumference offset or temporal change will result in an effective frequency error. This is accompanied by a fixed offset of the circumference of about 0.9 mm to account for the time of flight change from low to high energy resulting from the change in particle speed.

* patrick.schreiber@synchrotron-soleil.fr

Table 1: Main Parameters for the Upgraded Booster

Parameter	Unit	Value
Circumference	m	156.46
Natural Emittance	nm · rad	5.2
Betatron Tunes		13.190, 4.185
Chromaticities		1, 1
Energy	GeV	0.15 – 2.75
RMS Bunch Length	ps	25@3 MV
Repetition Frequency	Hz	3

Table 2: Values for Errors Used in the Robustness Studies. Values Given Are Standard Deviations and Sampling of Errors from the Resulting Distributions Were Cut at 2σ. For the Simulations 250 Seeds Were Used

Source	Unit	Value
Girder Offset	µm	50
Girder Roll/Pitch/Yaw	µrad	100
Magnet Offset	µm	50
Magnet Roll/Pitch/Yaw	µrad	100
Magnet Calibration		0.001
BPM Offset	µm	500
BPM Roll	µrad	400
Circumference	mm	1
RF Frequency	kHz	2.5

As the beam is more stable at higher energy, the ring will be aligned with respect to injection energy resulting in an offset error at extraction energy. The applied corrections include orbit, tunes, chromaticities and coupling with 10 skew quadrupoles integrated in sextupoles. Robustness has also been studied for the storage ring [10]. The following studies were performed at extraction energy (2.75 GeV).

With the given errors, the robustness studies result in absolute orbit deviations of up to $O^{\mathrm{x}}_{\mathrm{max}} = 2.89$ mm horizontally and $O^{\mathrm{y}}_{\mathrm{max}} = 1.52$ mm vertically. These values, however, are mostly present in just a few seeds, which is why it is more meaningful to examine the 95$^{\mathrm{th}}$ percentile, where the machines with the top 5 % orbit deviations are excluded. Thus, the values for the orbit deviation are $O^{\mathrm{x}}_{95^{th}} = 2.36$ mm and $O^{\mathrm{y}}_{95^{th}} = 1.25$ mm.

The horizontal beta-beat induced by these errors is shown in Fig. 1. The significantly high values in horizontal beta-beat and orbit result from the time-of-flight problem and the error on the frequency of the RF system. Both of those points induce an energy error forcing the beam to follow the dispersion inducing the observed high values. As the frequency of the RF system is mandated by the storage ring

ISBN: 978-3-95450-247-9 ISSN: 2673-5490 doi: 10.18429/JACoW-IPAC2024-THPC36

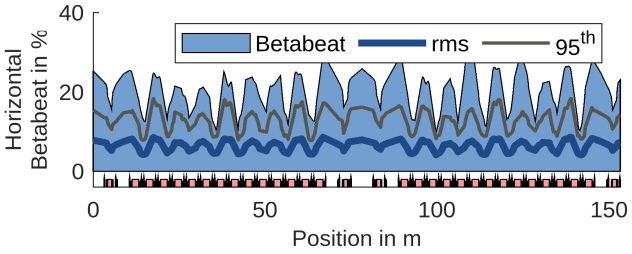

Figure 1: Horizontal beta-beat with all errors except power supply tracking errors. The blue area shows the maximum and the grey line shows the 95$^{\text{th}}$ percentile.

there is no possibility to reduce this energy error and further options to reduce beta-beat, e.g. through LOCO, are not feasible with the quadrupole magnets powered in families.

The required dipolar corrector angle $D^{x/y}$ are below $D^{\text{x}}_{\text{max}} = 0.28$ mrad and $D^{\text{y}}_{\text{max}} = 0.28$ mrad. Similar to the orbit, these strengths are only required for a few seeds and the 95$^{\text{th}}$ percentile is a valid metric where the strengths are below $D^{\text{x}}_{95^{th}} = 0.25$ mrad and $D^{\text{y}}_{95^{th}} = 0.24$ mrad. With the correctors in the arc integrated in sextupoles with a length of 21.2 cm this value is well within feasibility limits. The correctors in the straight sections are shorter standalone magnets within an available space of 90 mm. The required strength for these magnets is below $D^{\text{x}}_{95^{th}} = 0.23$ mrad and $D^{\text{y}}_{95^{th}} = 0.15$ mrad and again within feasibility limits.

TRACKING ERRORS

Small imperfections of the power supplies and their timing result in slightly different magnet strengths for each ramping cycle. The induced errors on the strength are referred to as *tracking* errors. For the SOLEIL II booster, 15 power supplies for the main magnets are planned. Additionally, the corrector magnets will be individually powered and ramped as well. The power supplies exhibit independent tracking errors which results in errors of the optics which can not be corrected due to the shot-by-shot nature of these errors.

One of the most obvious metrics showing the effect of the tracking errors is the tune. For two different levels of tracking error, the tune is shown in Fig. 2. The tracking error is specified as an error on the magnet strength as a fraction of the nominal strength. The shown tunes correspond to tracking error levels $\sigma_{\text{T}} = 0.3 \times 10^{-3}$ and $\sigma_{\text{T}} = 0.05 \times 10^{-3}$. The nominal machine without errors is tuned to a working point of $(\nu_{\text{x}}, \nu_{\text{y}}) = (0.19, 0.185)$. For $\sigma_{\text{T}} = 0.3 \times 10^{-3}$ and this working point, the tracking errors are large enough for the resulting spread in tunes to cross the coupling resonance. This is too much, especially when considering the resonance crossing described below. For the lower value of $\sigma_{\text{T}} = 0.05 \times 10^{-3}$, the tune spread resulting from tracking errors is significantly lower and much less of a problem.

First internal tests of the expected stability of the foreseen power supplies using new FGC controllers from CERN show an expected performance around $\sigma_{\text{T}} = 0.05 \times 10^{-3}$.

The tracking error also has an effect on other parameters such as beta-beat. The impact of tracking errors with a level

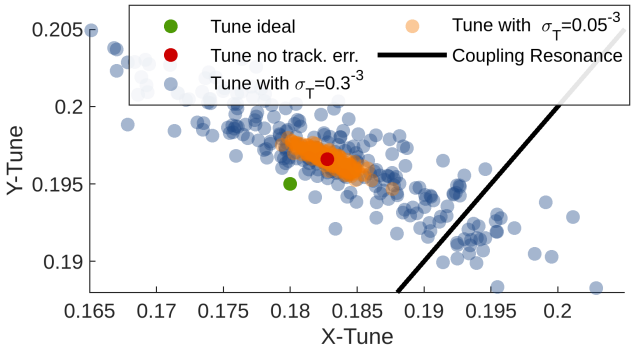

Figure 2: Spread of the tune for one sample machine with average orbit deviations after corrections. Blue dots show the tune spread for a tracking error of σ_{T}=0.3 × 10^{-3} and orange dots for σ_{T}=0.05 × 10^{-3}. The red dot represents the tune of the corrected sample machine without tracking errors and the green dot marks the ideal tune of (0.18, 0.195). The coupling resonance is shown as black line.

of $\sigma_{\text{T}} = 0.3 \times 10^{-3}$ is significant with an increase from 31 % up to 57 %. On the other hand, with the lower level of $\sigma_{\text{T}} = 0.05 \times 10^{-3}$, the impact of tracking errors is negligible and they increase the beta-beat by only 0.8 %.

EMITTANCE EXCHANGE

For a 100 % injection rate into the new storage ring a small horizontal emittance may be beneficial, depending on the performance of horizontal and vertical dynamic aperture of the storage ring in the future. Therefore, emittance exchange options were evaluated for the booster upgrade.

An exchange in the transfer line from booster to storage ring has been discarded due to space requirements. Generally two methods for emittance exchange can be considered [11, 12], resonance crossing and by means of a pulsed skew quadrupole. The effectiveness of resonance crossing has been previously shown (e.g. [11]). To evaluate this method for the SOLEIL II booster a machine with errors after correction was chosen that exhibits an orbit offset closest to the average of 250 seeds of errors after correction. The resonance crossing was optimised in terms of crossing speed and machine coupling. To control the coupling in simulations, a weak skew quadrupole in a straight section without dispersion was used. The simulation was done by tracking a matched bunch for about 1500 turns while changing the tune at each turn in 6D with radiation damping and quantum excitation. For this two families of quadrupoles were used to change the tunes at each turn. The resulting emittances are shown in Fig. 3.

A significant exchange can be observed with the best result at turn around 800. However, the emittance is oscillating quite significantly. Combined with the tracking errors described previously, which varies the tune before the exchange, the optimal extraction turn is varying significantly. The horizontal emittance for three example shots with different tunes caused by tracking errors is shown in Fig. 4. It is not possible to select a fixed extraction time with acceptable

ISBN: 978-3-95450-247-9 ISSN: 2673-5490 doi: 10.18429/JACoW-IPAC2024-THPC36

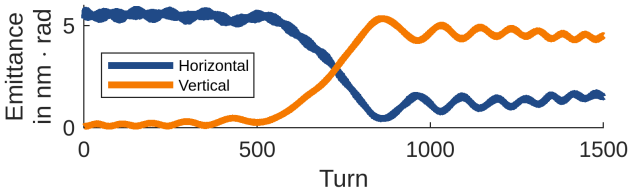

Figure 3: Emittances over turns for the resonance crossing option of emittance exchange. A significant exchange is happening but the emittances after the exchange oscillate.

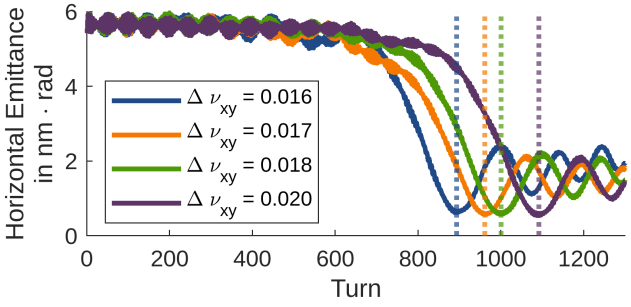

Figure 4: Horizontal emittance during the emittance exchange for three different starting tunes. The difference in tune is caused by the tracking error as described above.

horizontal emittance. As the shot-to-shot stability would result in a significant variation in emittance, the resonance crossing method is not suitable for the upgraded booster.

The second method is emittance exchange with a pulsed skew quadrupole. This method uses a fast pulsed skew quadrupole in the long straight section with no dispersion. The height and length of the pulse have been optimised for an ideal machine and the exchange was later studied for 250 machines with errors and corrections applied. Figure 5 shows the applied pulse with a length of 2.6 µs. Figure 6a shows a histogram of the horizontal emittance before and after the exchange. While the distribution is not perfect, the final horizontal emittance is mostly distributed around 0.5 nm rad. The impact of the tracking errors seem to be much smaller for this method than for resonance crossing. To evaluate the temporal, i.e. injection shot-to-shot, jitter, a single seed of static errors was evaluated with 250 seeds of tracking errors. The seed of static errors was chosen to be as close in orbit deviation to the average of 250 seeds as possible. The resulting distribution is shown in Fig. 6b. A narrow distribution even below 0.5 nm rad is visible.

For both methods correction of the machine coupling is required. Resonance crossing requires a tight control of the machine coupling, while for the pulsed skew quadrupole method the coupling should be as low as possible.

CONCLUSION

The robustness studies showed, that the non-correctable effects induced by the frequency error of the RF system as well as the energy offset caused by the time-of-flight offset at high energy have a significant impact on robustness. However, even with these effects, the required strength of the dipolar correctors is within feasible ranges and the lattice can be corrected to acceptable levels. In terms of emittance exchange, two methods were studied, resonance crossing and a pulsed skew quadupole. The resonance crossing method shows high susceptibility to tracking errors and exhibits a large distribution of final horizontal emittances after the exchange which is too large for efficient exchange. The pulsed skew quadrupole method, on the other hand, is sufficiently stable under tracking errors and also performs better otherwise. Therefore for the upgrade of the SOLEIL booster the pulsed skew quadrupole method is favoured. The next major step for the evaluation of the SOLEIL II booster will be detailed commissioning simulations to assess feasibility of commissioning the machine.

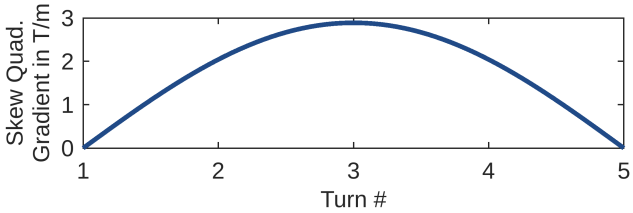

Figure 5: Pulse shape for the emittance exchange using a fast pulsed skew quadrupole.

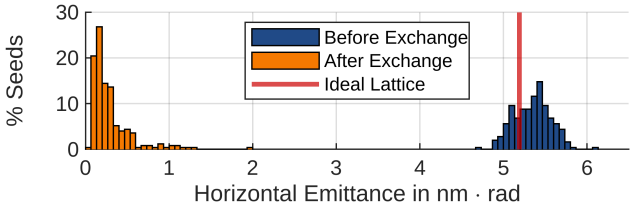

(a) Data for 250 seeds of errors after correction with tracking errors.

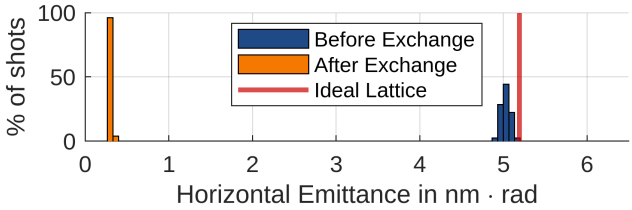

(b) Data for 250 shots for a single set of static errors.

Figure 6: Histogram of the horizontal emittance before and after emittance exchange with a pulsed skew quadrupole. Tracking errors were applied with $\sigma_T = 0.05 \times 10^{-3}$. Upper plot shows the performance for different seeds of static errors and lower plot shows the performance for one seed of static errors and 250 seeds of tracking errors to simulate the temporal injection shot-to-shot behaviour.

ACKNOWLEDGEMENTS

The authors would like to thank Liu Lin, LNLS for bringing the time of flight offset to our attention.

ISBN: 978-3-95450-247-9 ISSN: 2673-5490 doi: 10.18429/JACoW-IPAC2024-THPC36

REFERENCES

[1] J. Susini *et al.*, "A brief introduction to the Synchrotron SOLEIL and its upgrade programme," *The European Physical Journal Plus*, vol. 139, no. 1, p. 80, Jan 2024. doi:10.1140/epjp/s13360-024-04872-2

[2] A. Nadji and L. S. Nadolski, "Upgrade Project of the SOLEIL Accelerator Complex," *Synchrotron Radiation News*, vol. 36, no. 1, pp. 10–15, Apr. 2023. doi:10.1080/08940886.2023.2186661

[3] A. Loulergue *et al.*, "TDR baseline lattice for SOLEIL II upgrade project", in *Proc. IPAC'23*, Venice, Italy, May 2023, pp. 1054–1056. doi:10.18429/JACoW-IPAC2023-MOPM031

[4] M.-A. Tordeux *et al.*, "Injection Schemes for the SOLEIL Upgrade", in *Proc. IPAC'21*, Campinas, Brazil, May 2021, pp. 796–798. doi:10.18429/JACoW-IPAC2021-MOPAB248

[5] M.-A. Tordeux, Z. H. Bai, G. Liu, A. Loulergue, R. Nagaoka, and T. Zhang, "A Low-emittance Booster Lattice Design for the SOLEIL Upgrade", in *Proc. IPAC'21*, Campinas, Brazil, May 2021, pp. 410–413. doi:10.18429/JACoW-IPAC2021-MOPAB113

[6] M.-A. Tordeux *et al.*, "Progress on the New Booster for SOLEIL II", in *Proc. IPAC'23*, Venice, Italy, May 2023, pp. 3267–3271. doi:10.18429/JACoW-IPAC2023-WEPL072

[7] A. Terebilo, "Accelerator Toolbox for MATLAB", SLAC National Accelerator Lab., Menlo Park, United States, Rep. SLAC-PUB-8732, May 2001. doi:10.2172/784910

[8] Accelerator Toolbox Documentation, https://atcollab.github.io/at/m/index.html

[9] Toolkit for Simulated Commissioning Webpage, https://sc.lbl.gov

[10] O. Blanco-García, A. Loulergue, L. Nadolski, R. Nagaoka, and M.-A. Tordeux, "Status of the SOLEIL II robustness studies", in *Proc. IPAC'23*, Venice, Italy, May 2023, pp. 3263–3266. doi:10.18429/JACoW-IPAC2023-WEPL070

[11] J. Kallestrup and M. Aiba, "Emittance exchange in electron booster synchrotron by coupling resonance crossing", *Physical Review Accelerators and Beams*, vol. 23, no. 2, p. 020701, Feb. 2020. doi:10.1103/PhysRevAccelBeams.23.020701

[12] P. Kuske and F. Kramer, "Transverse Emittance Exchange for Improved Injection Efficiency", in *Proc. IPAC'16*, Busan, Korea, May 2016, pp. 2028–2031. doi:10.18429/JACoW-IPAC2016-WEOAA01